

Supplementary Information: Polarization interferometry for real-time spectroscopic plasmonic sensing

Lauren M. Otto¹, Daniel A. Mohr^{1,2}, Timothy W. Johnson¹, Sang-Hyun Oh¹, and Nathan C. Lindquist^{2,+}

¹Department of Electrical and Computer Engineering, University of Minnesota, Minneapolis, MN 55455, USA

²Physics Department, Bethel University, St. Paul, MN 55112, USA

⁺email: n-lindquist@bethel.edu

ALTERNATE STRUCTURE

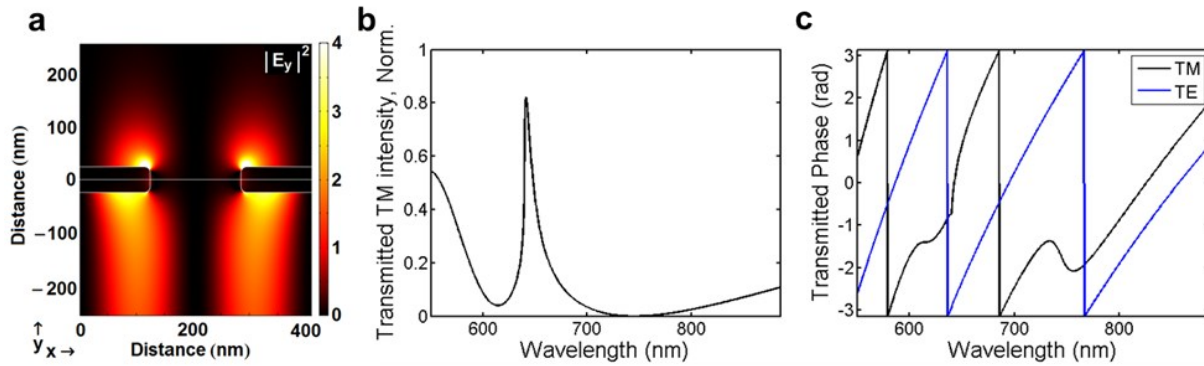


Figure S1: COMSOL modeling for slits in a 45 nm gold film, periodicity 410 nm, slit width 160 nm. (a) Field intensity map at the transmission maximum 641 nm. (b) TM mode transmitted intensity spectrum. (c) Transmitted phase. The periodic slit structure shows phase features that can be used with the measurement technique demonstrated in this paper. While the phase features are larger in width for this slit structure in comparison to our buried grating structure, further optimization could yield stronger effects.

A periodic slit structure with similar dimensions to our buried grating structure was modeled with COMSOL as a proof-of-concept for application of the presented measurement technique with structures other than our buried gratings. The modeling parameters were the same as in the buried grating model (described below), except the S21 parameters were extracted for the transmitted intensity and transmitted phase information. The light is incident from the bottom of the window (epoxy) and transmits through the slit and the top of the window (water).

DEVICE FABRICATION

A silicon wafer was cleaned with BOE followed by a one-to-one mixture of hydrogen peroxide and sulfuric acid to grow a smooth native oxide layer. A 19 nm gold layer was deposited using electron beam metal evaporation (CHA). PMMA (A4 950) was spin coated on the surface, electron beam lithography was performed, and the sample was developed for 35 sec (MIBK:IPA 1:3) yielding the grating patterns. A final 45 nm gold layer was evaporated onto the surface and a liftoff process using acetone was performed. The final structure was then removed from the silicon wafer with the “template stripping” method¹ using an optical adhesive (NOA 61) and a glass slide. A scanning electron micrograph (Figure 2b) post template stripping shows a single line grating, and an optical micrograph (Figure 2c) shows a small array of different gratings with both different periods and grating line widths.

DEVICE MODELING

Finite element method (FEM) simulations were conducted using COMSOL Multiphysics™ 4.4. The RF module was used along with a 2D grating unit cell and periodic boundary conditions. Simulations were conducted for both TE and TM polarizations, with and without the grating bump for data normalization (the mesh elements were kept identical for both geometries), and for both water and ethanol. The resulting reflected intensity and reflected phase spectra were extracted from the S-11 parameters. The light is incident from the bottom of the window (epoxy) and reflects off the grating.

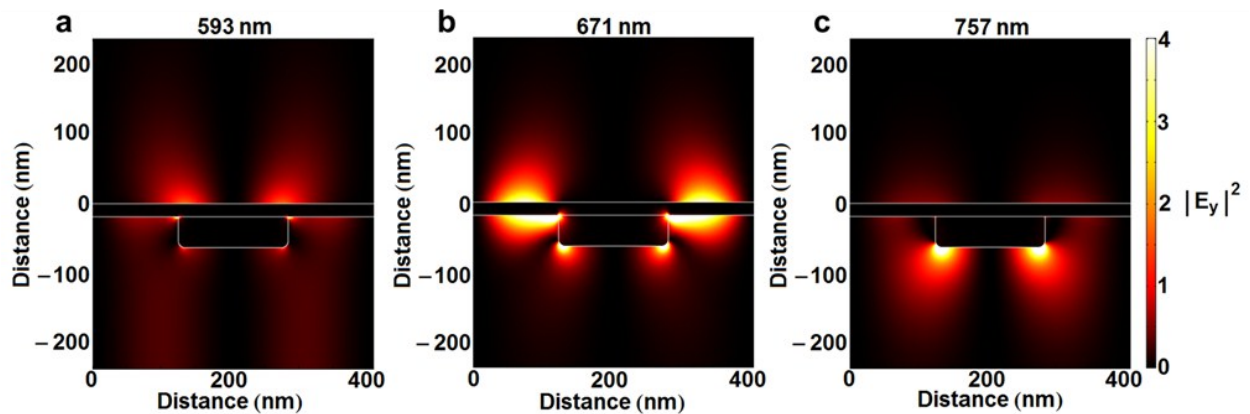


Figure S2: Field intensity maps shown for the modeled buried grating shown in Figure 3 (period 410 nm, line width 160 nm) at the three described resonance dips: (a) the “upper” side resonance at 593 nm, (b) the “coupled” resonance at 671 nm, and (c) the “buried” side resonance at 757 nm. All field maps are comparable to what was previously demonstrated².

ANALYSIS

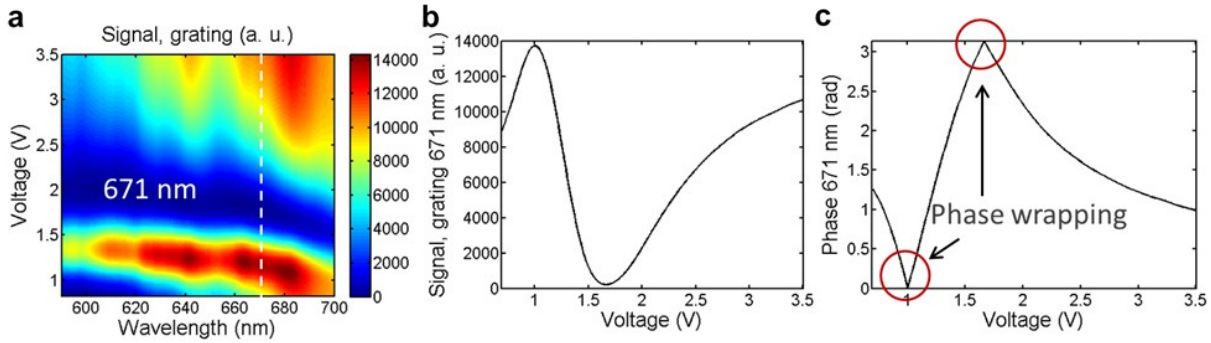


Figure S3: (a) The saved spectra from the grating region for one voltage scan. At each wavelength, Equation 1 is used to transform the signal curve (b) by centering it between +1 and -1 and using an *arccos* function to output the phase information (c).

As described in the main text, I_{max} and I_{min} are used in Equation 1 to center the data between +1 and -1 so that the *arccos* function can be used to determine the reflected phase³ (wrapped) due to the gratings (Figure S3c) and also the gold surface. Our homemade LabVIEW software enables the saving of spectra from both the grating and the gold surface simultaneously, and stores the voltage scan data in a matrix (Figure S3a). MATLAB code was used to analyze each wavelength of interest individually as the applied voltage was changed (Figure S3b,c).

INTENSITY SPECTRUM

With the same MATLAB script as was used to extract the phase spectra, we extracted the TM reflected intensity spectrum from the real-time data (Figure 5e,f) and from the real-time scan data (Figure 5b). The extracted spectra (water and 8.65 wt. % glycerol solution) are resulting from incident light polarized at 45 degrees (Figure S4d) and are compared with: (1) a set of spectra from 45 degree polarization measured directly (Figure S4c), without the LCVWP and the second polarizer in the light path, (2) a set of spectra from TM polarization measured directly (Figure S4b), without the LCVWP and the second polarizer in the light path, and (3) a set of spectra from TM polarization simulated by COMSOL. The two directly measured sets of spectra indicate the differences we expect to see between TM and 45 degree polarized light, *i.e.* the differences we expect to see between the spectra from COMSOL and the spectra derived from the scans our measurement system completes. The good agreement demonstrates the power of our measurement technique in that we are able to measure both phase and intensity quantitatively.

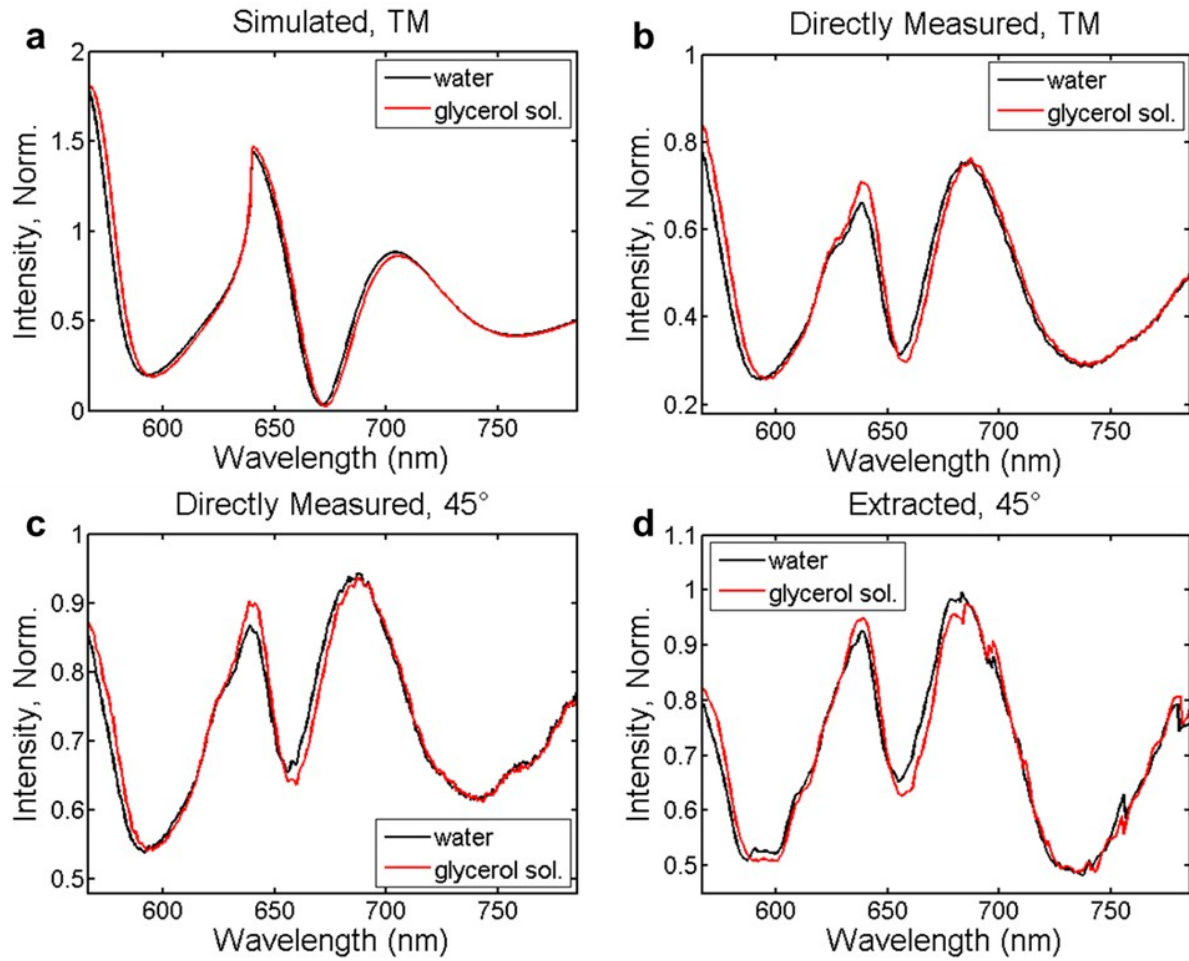


Figure S4: Reflected intensity spectra from (a) COMSOL with TM polarization, (b) direct measurement with TM polarization and (c) direct measurement with 45 degree polarization, both without the LCVWP and second polarizer in the optical path, and (d) extraction from the same real-time scans plotted in Figure 5b and performed with the presented measurement technique.

FWHM CALCULATIONS

The full width at half maximum (FWHM) was calculated in the same way for all phase and intensity features discussed in the paper. It is important to note that, as shown in Figure S5, the maximum was chosen as the lower of the two peaks surrounding our tracked dip feature.

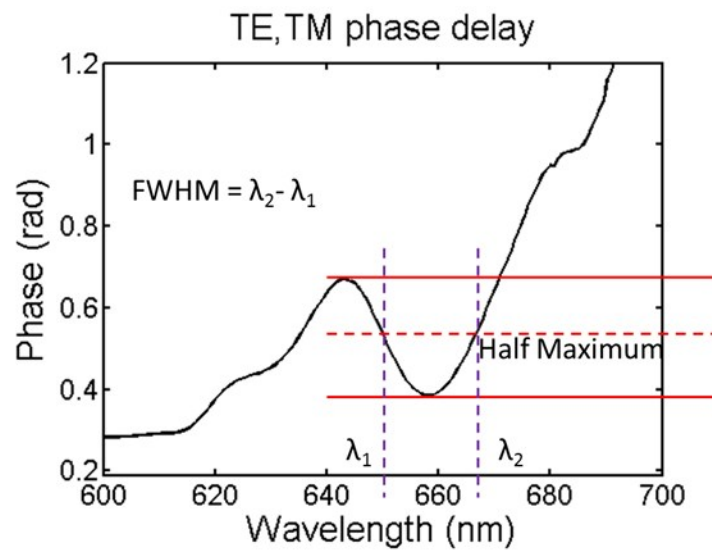


Figure S5: FWHM calculation demonstration.

REFERENCES

1. P. Nagpal, N. C. Lindquist, S.-H. Oh, and D. J. Norris, *Science*, 2009, **325**, 594–597.
2. N. C. Lindquist, T. W. Johnson, J. Jose, L. M. Otto, and S.-H. Oh, *Ann. der Phys.*, 2012, **524**, 687–696.
3. X. Zhang, M. Davanço, K. Maller, T. W. Jarvis, C. Wu, C. Fietz, D. Korobkin, X. Li, G. Shvets, and S. R. Forrest, *Opt. Express*, 2010, **18**, 17788–17795.